SUPPLEMENTAL MATERIALS AND METHODS

Histology

The orientation of tumors was marked before fixation in 4 % paraformaldehyde and subsequent embedding in paraffin. Transverse 5 µm sections were cut at the largest tumor diameter. Hematoxylin and eosin (H&E) staining was performed according to standard protocols.

Sections were incubated overnight at 4 °C with primary antibodies and for 1 hour at room temperature with respective secondary antibodies (see Supplemental Table 1 for antibody details). Cell death was detected by a commercially available kit (In situ TUNEL kit assay, Roche).

Stainings were evaluated using a Nikon Eclipse 90i fluorescent microscope and the NIS-Elements software package (Nikon). For quantification of Ki67 and BrdU staining 5 images at 20x resolution were acquired in regions with the highest fraction of specifically stained cells to compare the labeling index to radiotracer uptake expressed as $\%ID_{max}$/mL. Numbers of stained nuclei were determined using the software Fiji (ImageJ). For quantifying TUNEL or caspase-3 staining, 5 representative images in the proliferative regions of the tumor were chosen.

Western Blot

Excised tumors were frozen in liquid nitrogen and the tissue was homogenized by a micro-dismembrator. Proteins were denatured in RIPA buffer (Cell Signaling) and subjected to western blot analysis. The nitrocellulose membrane was incubated overnight at 4 °C with specific primary antibodies. Afterwards the membrane was probed with appropriate peroxidase-coupled secondary antibodies for 1 hour at room temperature (see Supplemental Table 1 for antibody details). Protein bands were visualized with the Pierce ECL Plus Western Blotting Substrate (Pierce Biotechnology).

Thymidine Analysis

A liquid-chromatography—mass spectrometry (LC-MS/MS) method for the quantitative analysis of thymidine in tumor tissue homogenate was developed by the PK/Bioanalytics Core Facility at the CRUK Cambridge Institute. Briefly, thymidine quantification of tissue homogenates was made against calibration standards prepared with authentic reference standards of thymidine. All results quoted are from batches in which calibration standards and quality controls were within the acceptance criteria of ± 15 % relative error for at least 75 % of standards and quality controls.

SUPPLEMENTAL TABLES:

Supplemental Table 1:

Antibodies used for immunohistochemistry (IHC) and western blot (WB)

primary antibodies				**dilution factor**	
antigen	**host**	**source**	**clone / order number**	**IHC**	**WB**
actin	mouse	MP Biomedicals	clone C4, 69100		1:1000
active caspase-3	rabbit	BD Pharmingen	CPP-32, Clone C92-605	1:100	
BrdU	rat	AbD Serotech	OBT0030G	1:100	
human SLC29A1/ENT1	rabbit	Acris	11337-1-AP	1:100	1:1000
Ki67	rabbit	Abcam	ab16667	1:100	
thymidylate synthase	rabbit	Abcam	ab108995	1:50	1:1000
thymidine kinase 1	rabbit	Abcam	EPR3193	1:200	1:1000
thymidine phosphorylase	rabbit	Acris	12383-1-AP	1:50	1:1000
thymidylate synthase	rabbit	Abcam	ab108995	1:50	1:1000

secondary antibodies				**dilution factor**	
antigen	**species**	**label**	**source**	**IHC**	**WB**
mouse	rabbit	peroxidase	Dako		1:4000
rabbit	donkey	biotin	Amersham	1:200	
rabbit	goat	Alexa Fluor 488	Life Technologies	1:1000	
rabbit	goat	biotin	Invitrogen	1:500	
rabbit	goat	peroxidase	Dako		1:2000

Supplemental Table 2:

Absolute values of the bar charts shown in Fig. 2, 3, 6, 7 and Supplemental Fig. 1, 3, 4*

Parameter	A549	HTB56	EBC1	H1975
Figure 2: ^{18}F-FDG and ^{18}F-FLT small-animal PET imaging				
FDG (%ID$_{max}$/mL)	3.5 ± 1.2	5.5 ± 1.0	4.4 ± 1.4	6.1 ± 2.7
FLT (%ID$_{max}$/mL)	8.5 ± 3.2	4.4 ± 0.7	4.4 ± 1.2	12.1 ± 3.5
Figure 3: Histology of proliferation markers				
Ki67 index (%)	39.6 ± 7.5	72.5 ± 4.9	59.2 ± 9.6	31.5 ± 9.6
BrdU index (%)	9.4 ± 2.1	24.7 ± 1.3	26.0 ± 8.7	18.8 ± 4.5
Fig. 6: Small-animal MR imaging				
Mean viable ADC (10^{-3} mm^2/s)	0.973 ± 0.079	0.725 ± 0.107	0.763 ± 0.089	1.100 ± 0.206
Fig. 7: Histology of cell death				
Caspase-3-positive nuclei (%)	2.9 ± 2.0	16.0 ± 6.9	10.7 ± 9.2	5.3 ± 2.7
TUNEL-positive nuclei (%)	0.5 ± 0.4	3.6 ± 2.9	1.9 ± 1.3	0.9 ± 0.6
Supplemental Fig. 1: ^{18}F-FDG and ^{18}F-FLT small-animal PET imaging - various quantifications				
FDG (tumor-muscle ratio)	4.3 ± 1.6	6.3 ± 1.1	5.9 ± 2.3	7.7 ± 2.8
FDG (tumor-liver-ratio)	2.3 ± 1.1	2.6 ± 0.9	3.4 ± 1.3	4.0 ± 2.2
FDG (SUV$_{max}$)	1.0 ± 0.3	1.5 ± 0.3	1.2 ± 0.4	1.6 ± 0.6
FDG (%ID$_{mean}$/ml)	2.0 ± 0.6	2.5 ± 0.6	2.1 ± 0.4	2.5 ± 1.0
FLT (tumor-muscle ratio)	4.0 ± 1.5	2.2 ± 0.6	2.3 ± 0.8	6.5 ± 2.1
FLT (tumor-liver ratio)	3.1 ± 1.0	1.7 ± 0.3	1.7 ± 0.4	4.9 ± 1.4
FLT (SUV$_{max}$)	2.2 ± 0.8	1.2 ± 0.2	1.2 ± 0.3	3.4 ± 1.0
FLT (%ID$_{mean}$/ml)	3.6 ± 0.8	2.4 ± 0.4	2.4 ± 0.5	3.8 ± 1.3
Supplemental Fig. 3: Tumor thymidine				
Thymidine (µM)	3.7 ± 4.0	11.1 ± 0.8	13.1 ± 3.4	3.7 ± 1.6
Supplemental Fig. 4: Cellular density				
Nuclei per FOV	1,087 ± 142	1,339 ± 192	1,078 ± 236	663 ± 119

* mean ± SD

Supplemental Table 3:

Statistical analysis of bar charts in Fig. 2, 3, 6, 7 and Supplemental Fig. 1, 3, 4*

Parameter	A549 vs HTB56	A549 vs EBC1	A549 vs H1975	HTB56 vs H1975	HTB56 vs EBC1	EBC1 vs H1975
Fig. 2: ^{18}F-FDG and ^{18}F-FLT small-animal PET imaging						
FDG (%ID$_{max}$/ml)	s.	n.s.	s.	n.s.	s.	s.
FLT (%ID$_{max}$/ml)	s.	s.	s.	s.	n.s.	s.
Fig. 3: Histology of proliferation markers						
Ki67 index	s.	s.	n.s.	s.	s.	s.
BrdU index	s.	s.	n.s.	n.s.	n.s.	n.s.
Fig. 6: Small-animal MR imaging						
ADC	s.	s.	n.s.	s.	n.s.	s.
Fig. 7: Histology of cell death						
TUNEL	s.	s.	n.s.	s.	s.	s.
Caspase-3	s.	s.	n.s.	s.	n.s.	n.s.
Supplemental Fig. 1: ^{18}F-FDG and ^{18}F-FLT small-animal PET imaging – various quantifications						
FDG (tumor-muscle ratio)	s.	s.	s.	n.s.	n.s.	s.
FDG (tumor-liver-ratio)	n.s.	s.	s.	s.	n.s.	n.s.
FDG (SUV$_{max}$)	s.	n.s.	s.	n.s.	s.	s.
FDG (%ID$_{mean}$/ml)	n.s.	n.s.	n.s.	n.s.	n.s.	n.s.
FLT (tumor-muscle ratio)	s.	s.	s.	s.	n.s.	s.
FLT (tumor-liver ratio)	s.	s.	s.	s.	n.s.	s.
FLT (SUV$_{max}$)	s.	s.	s.	s.	n.s.	s.
FLT (%ID$_{mean}$/ml)	s.	s.	n.s.	s.	n.s.	s.
Supplemental Fig. 3: Tumor thymidine						
Thymidine	s.	s.	n.s.	s.	n.s.	s.
Supplemental Fig. 4: Cellular density						
Nuclei per FOV	n.s.	n.s.	s.	s.	n.s.	s.

* One way ANOVA (Holm-Sidak method), s.: significant (P-values ≤0.05), n.s.: non significant

SUPPLEMENTAL FIGURES:

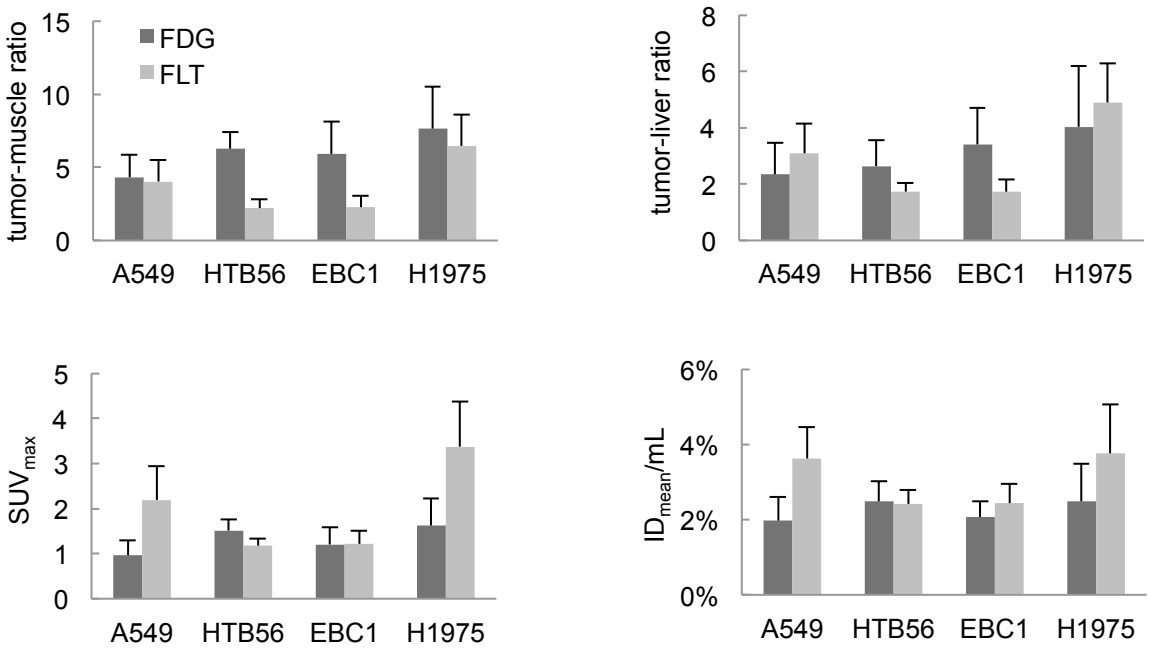

Supplemental Figure 1: Different quantification methods of PET parameters reveal similar differences of ^{18}F-FDG and ^{18}F-FLT uptake in lung carcinoma xenografts. Small-animal PET images were not only quantified as maximum radiotracer uptake (%ID$_{max}$/mL, Fig. 2) but also other methods of quantification were used as described in materials and methods. All analysis methods show that ^{18}F-FDG uptake is within a comparable range in all xenografts (see also Supplemental Table 2). ^{18}F-FLT was elevated in A549 and H1975 xenografts irrespective of the quantification mode. The number of tumors analyzed is the same as in Fig. 2.

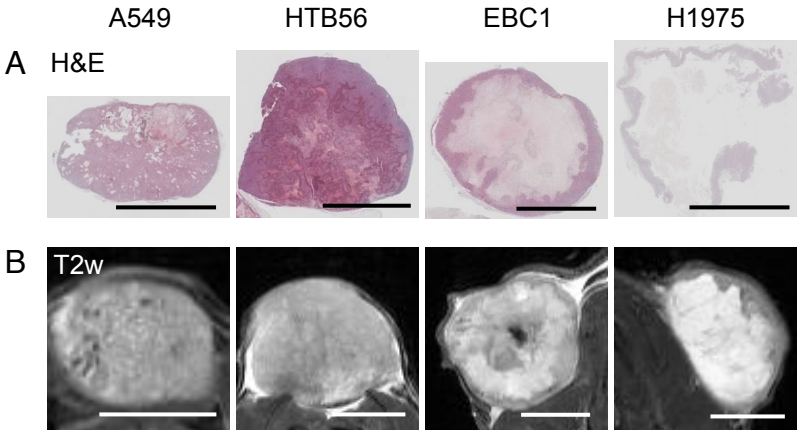

Supplemental Figure 2: Variability of lung cancer xenografts in terms of morphology. Hematoxylin and eosin (H&E) staining (A) and T2w in vivo MR imaging (B) of the same tumors demonstrate that the investigated tumors types differ with respect to anatomy, for example presence of tumor stroma and edema. Transverse sections of representative tumors at biggest tumor diameter are shown here. MR imaging was performed 4 wk after tumor inoculation, before tumors were excised for histological analysis. Scale bars = 5 mm.

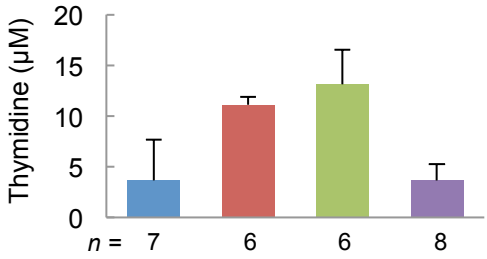

Supplemental Figure 3: Thymidine concentrations differ between various lung cancer xenografts. The presented bar graph shows the average thymidine concentrations of the 4 investigated xenografts as determined by a thymidine specific LC-MS/MS analysis. Blue = A549, red = HTB56, green = EBC1, purple = H1975. *n* = number of tumor lysates analyzed per cell line.

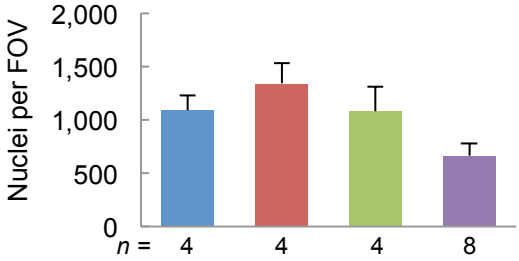

Supplemental Figure 4: Lung cancer xenografts vary with respect to cellular density. The number of DAPI stained nuclei per field of view (FOV, 20x resolution, 580 x 460 µm) was determined as a measure for cellular density. Blue = A549, red = HTB56, green = EBC1, purple = H1975. *n* = number of tumors analyzed per cell line.